

Douglas du Boulay,\* Akito  
Sakaguchi, Katsumi Suda and  
Nobuo IshizawaMaterials and Structures Laboratory, Tokyo  
Institute of Technology, 4259 Nagatsuta Midori,  
Yokohama 226-8503, JapanCorrespondence e-mail:  
ddb@r3401.msl.titech.ac.jp

## Key indicators

Single-crystal X-ray study  
 $T = 293\text{ K}$   
Mean  $\sigma(\text{Li-O}) = 0.003\text{ \AA}$   
 $R$  factor = 0.033  
 $wR$  factor = 0.026  
Data-to-parameter ratio = 32.7For details of how these key indicators were  
automatically derived from the article, see  
<http://journals.iucr.org/e>.Reinvestigation of  $\beta\text{-Li}_3\text{TaO}_4$ 

The structure of  $\beta\text{-Li}_3\text{TaO}_4$  has been reinvestigated with an image plate diffractometer. It crystallizes with a cation-ordered, distorted rock-salt-type lattice structure, composed of distorted  $\text{TaO}_6$  and  $\text{LiO}_6$  octahedra. Some evidence of a superlattice was observed, but it had no impact on the established structural model.

Received 9 April 2003  
Accepted 22 April 2003  
Online 30 April 2003

## Comment

Miao and Toradi (1999) have explored the X-ray luminescence properties of the  $\text{Li}_3\text{Ta}_{1-x}\text{Nb}_x\text{O}_4$  phase diagram and identified a promising phosphor candidate for medical X-ray and UV imaging detectors. When the  $\beta\text{-Li}_3\text{TaO}_4$  lattice is doped with Nb in the composition range  $0.001 < x < 0.01$ , the normal  $\text{Li}_3\text{TaO}_4$  broadband blue luminescence becomes concentrated, and peaks at around 415 nm with an intensity comparable to that of some commercial phosphors. The luminescence efficiency rapidly declines with increasing Nb concentration and presumably increased lattice strain, which changes the photonic coupling of the substrate to the Nb ion fluorescence centres.

$\beta\text{-Li}_3\text{TaO}_4$  crystallizes in a structure resembling that of common rock salt (Fig. 1). It contains a well ordered Li and Ta cation sublattice (Mather *et al.*, 2000), organized as edge-sharing  $\text{LiO}_6$  and  $\text{TaO}_6$  octahedra. The  $\text{TaO}_6$  octahedra form distinct continuous chains, each edge being shared with two other  $\text{TaO}_6$  octahedra (Figs. 2 and 3). The octahedral chains

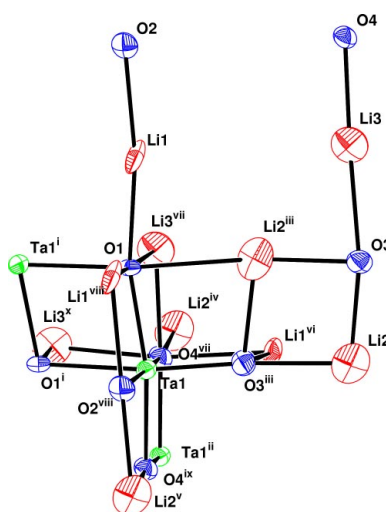
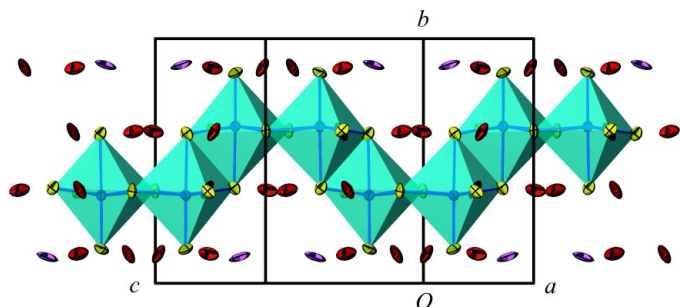


Figure 1

90% probability level ORTEP (*Xtal3.7*; Hall *et al.*, 2000) plot of extended asymmetric unit. [Symmetry codes: (i)  $-x, y, \frac{1}{2} - z$ ; (ii)  $-x, -y, -z$ ; (iii)  $1 - x, y, \frac{1}{2} - z$ ; (iv)  $-\frac{1}{2} + x, \frac{1}{2} + y, z$ ; (v)  $\frac{1}{2} - x, -\frac{1}{2} - y, -z$ ; (vi)  $x, -y, -\frac{1}{2} + z$ ; (vii)  $1 - x, -y, 1 - z$ ; (viii)  $\frac{1}{2} - x, -\frac{1}{2} - y, 1 - z$ ; (ix)  $-1 + x, y, -1 + z$ ; (x)  $-1 + x, -y, -\frac{1}{2} + z$ .]



**Figure 2**  
An *ATOMS* (Dowty, 1999) polyhedral view of the structure projected along the crystallographic *c* axis (O atoms yellow; Li red and pink). Displacement ellipsoids are drawn at the 90% probability level.

zigzag back and forth with a spatial repetition period of four octahedral units. The Li cations then occupy the considerably distorted  $\text{LiO}_6$  octahedra which envelop and separate the Ta-containing chains. Twofold axes pass through the midpoints of one subset of  $\text{TaO}_6$  shared edges, while inversion centres are to be found on the other shared  $\text{TaO}_6$  edges, as well as on shared  $\text{LiO}_6$  octahedral edges.

Martel & Roth (1981) observed two phase transitions in the  $\text{Li}_3\text{TaO}_4$  system using differential thermal analysis, one at 1173 K and a second at around 1700 K. Zocchi *et al.* (1983) ascribed the low temperature  $\beta$ -form to a cell of dimensions  $a = 8.500$  (3),  $b = 8.500$  (3),  $c = 9.3443$  (3) Å,  $\beta = 117.05$  (2)° and space group  $C2/c$ . The high temperature  $\alpha$ -form was ascribed to  $a = 6.027$  (2),  $b = 6.004$  (2),  $c = 12.822$  (4) Å,  $\beta = 103.60$  (2)° and space group  $P2$ . Subsequently the  $\alpha$ -phase was revised to  $P2/n$  (Zocchi *et al.*, 1984). Roth (1984) suggested that there may be several intermediate polymorphs, including both disordered and metastable variants, though as yet these remain uncharacterized. Earlier structural reports of  $\text{Li}_3\text{TaO}_4$  were made by Lapicky & Simanov (1953), Blasse (1964), and Grenier *et al.* (1964); although those authors basically concur on the general lattice morphology, the actual symmetry and cell choices are invariably close approximations. Zocchi *et al.* (1983) explored the cation ordering with greater precision, using X-ray and neutron powder diffraction to study the  $\beta$ -form and single-crystal X-ray diffraction to study a quenched sample of the  $\alpha$ -phase.

Reinvestigation of a single crystal of the  $\beta$ -phase on an image plate diffractometer reveals a weakly scattering superlattice (see refinement details). We suspect that local structural disorder, for example in which the two-level zigzag chains in the (100) plane become locally three-level chains, with a lattice repeat of eight  $\text{TaO}_6$  units, can easily be accommodated by the lattice. However, the weak intensity and limited number of the superlattice reflections preclude a more quantitative analysis. The refined structural model indicates that the Li2-centred octahedron is strongly distorted, with two Li2–O bonds longer than 2.4 Å. However, bond valence sums calculated for the present model were 0.94, 0.97, and 0.95 for Li1, Li2, and Li3, respectively, and 4.97 for Ta, which appear quite consistent with formal  $\text{Li}^{+1}$  and  $\text{Ta}^{+5}$  cation configurations.

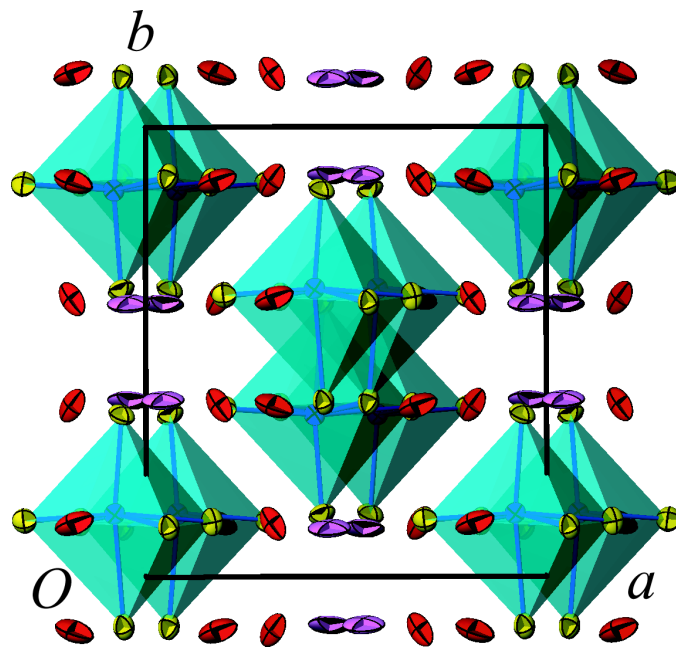


**Figure 3**  
Modulated  $\text{TaO}_6$  octahedral chains (*ATOMS*; Dowty, 1999) in the (100) plane. Displacement ellipsoids are drawn at the 90% probability level.

The refined atomic parameters converge to a sensible model that differs from the results of Zocchi *et al.* (1983) by up to the order of 15 of their s.u.s, which are typically larger than those in our work by a factor of at least 3. In addition, we report anisotropic displacement parameters for all atoms for the first time. The enhanced precision could be useful for future theoretical calculations of physical properties.

## Experimental

In a Pt crucible,  $\text{Li}_2\text{SO}_4 \cdot \text{H}_2\text{O}$  (0.574 mmol) and  $\text{Ta}_2\text{O}_5$  (0.191 mmol) with an additional 37.8 mmol of  $\text{Li}_2\text{SO}_4 \cdot \text{H}_2\text{O}$  flux were heated at 275 K  $\text{h}^{-1}$  to 1373 K, which was sustained for 5 h before cooling at 5 K  $\text{h}^{-1}$  to 723 K. The sample was discharged into room conditions and rinsed under water, revealing transparent colourless crystal blocks with sizes up to around  $0.24 \times 0.24 \times 0.28$  mm and a fine white powdery residue of  $\text{LiTaO}_3$ .

### Crystal data

$\text{Li}_3\text{TaO}_4$   
 $M_r = 265.77$   
Monoclinic,  $C2/c$   
 $a = 8.508$  (1) Å  
 $b = 8.516$  (1) Å  
 $c = 9.338$  (1) Å  
 $\beta = 116.869$  (10)°  
 $V = 603.54$  (13) Å<sup>3</sup>  
 $Z = 8$

$D_x = 5.85$  Mg  $\text{m}^{-3}$   
Mo  $K\alpha$  radiation  
Cell parameters from 63939 reflections  
 $\theta = 3.6$ – $69.9^\circ$   
 $\mu = 36.24$   $\text{mm}^{-1}$   
 $T = 293$  K  
Irregular block, colourless  
 $0.13 \times 0.12 \times 0.10$  mm

### Data collection

Rigaku Rapid image plate diffractometer  
 $\omega$  scans  
Absorption correction: numerical (*NUMABS*; Higashi, 2000)  
 $T_{\min} = 0.066$ ,  $T_{\max} = 0.237$   
10260 measured reflections

2422 independent reflections  
2269 reflections with  $F > 0.00\sigma(F)$   
 $R_{\text{int}} = 0.038$   
 $\theta_{\text{max}} = 45.3^\circ$   
 $h = -16 \rightarrow 16$   
 $k = -16 \rightarrow 16$   
 $l = -13 \rightarrow 18$

## Refinement

Refinement on  $F$   
 $R = 0.033$   
 $wR = 0.026$   
 $S = 3.03$   
 2422 reflections  
 74 parameters

$(\Delta/\sigma)_{\max} = 0.001$   
 $\Delta\rho_{\max} = 4.69 \text{ e } \text{Å}^{-3}$   
 $\Delta\rho_{\min} = -3.41 \text{ e } \text{Å}^{-3}$   
 Extinction correction: Zachariasen (1968)  
 Extinction coefficient: 138 (7)

A weakly scattering superlattice was identified that was fully indexed on a unit cell of dimensions  $a = 8.5$ ,  $b = 8.5$ , and  $c = 16.6 \text{ Å}$  with  $\alpha = \gamma = 90.0^\circ$  and  $\beta = 90.2^\circ$ . Apart from a small number of reflections (36 for the whole sphere), all located on the  $k = \pm 1$  plane (e.g. 011, 211, 013 etc), the superlattice exhibits nearly perfect  $B$  and  $C$  centring. The exceptions were all of low scattering angle, very weak, but significant and with reasonable Friedel pair agreement. The  $a$  and  $c$  lattice vectors used above match those reported by Zocchi *et al.* (1983) and the vector from the origin to the superlattice pseudo  $B$ -centre matches their  $c$  axis. The precise transformation we used to convert between them was  $a' = -a$ ,  $b' = -b$ ,  $c' = a/2 + c/2 = 9.338 \text{ Å}$ , with  $\beta = 116.874^\circ$ .

In adopting the smaller sublattice we have assumed that the small number of observed, but weak, pseudo- $B$ -centred reflections of the superlattice arose as artifacts of a minor degree of structural disorder, leading to some locally doubled  $c$ -axis. Although complicated twinning modes cannot be categorically excluded, the  $c = 16.6 \text{ Å}$  superlattice is pseudo-tetragonal, so simple twinning operations, such as the interchange of  $a$  and  $b$  (of the reduced cell), or twofold or mirror twinning operations about  $a$  and  $b$ , lead to pseudo-merohedral reflection superpositions and therefore should not give rise to the extra half  $c^*$  (of the reduced cell) superlattice reflections.

Although the  $wR(F)$ -factor of 0.026 is acceptable overall, some high and low angle weakly scattering reflection measurements were considerably stronger than their modelled values. Presumably this was associated with the twin or disorder component which we opted to ignore.

The deepest hole is located near the Ta1 atom nucleus. The highest peaks are coordinated pairwise  $0.545 \text{ Å}$  from the Ta1 atom. Starting coordinates adopted were those of Zocchi *et al.* (1983).

Data collection: *RAPID-AUTO* (Rigaku, 1999); cell refinement: *RAPID-AUTO* (Rigaku, 1999); data reduction: *RAPID-AUTO* and *DIFDAT ADDREF SORTRF* in *Xtal3.7* (Hall *et al.*, 2000); program(s) used to refine structure: *CRYLSQ* in *Xtal3.7*; molecular graphics: *ATOMS* (Dowty, 1999); software used to prepare material for publication: *BONDLA CIFIO* in *Xtal3.7*.

This study was supported by grants-in-aid for Scientific Research in Priority Areas (B) No. 740, and No. 14550663 from the Ministry of Education, Culture, Sports, Science and Technology, Japan. DDB acknowledges a grant-in-aid for JSPS fellows, No. P02148 from the Ministry of Education, Culture, Sports, Science and Technology, Japan.

## References

- Blasse, G. (1964). *Z. Anorg. Allg. Chem.* **331**, 44–50.  
 Dowty, E. (1999). *ATOMS for Windows*. Version 4.0. Shape Software, Kingsport, TN, USA.  
 Grenier, J. C., Martin, C. & Durif, A. (1964). *Bull. Soc. Fr. Miner. Crist.* **87**, 316–330.  
 Hall, S. R., du Boulay, D. J. & Olthof-Hazekamp, R. (2000). *Xtal3.7 System*. University of Western Australia, Australia. (<http://Xtal.crystal.uwa.edu.au/>)  
 Higashi, T. (2000). *NUMABS*. Rigaku Corporation, Tokyo, Japan.  
 Lapicky, A. V. & Simanov, Ju. P. (1953). *Struct. Rep.* **17**, 392–392.  
 Martel, L. C. & Roth, R. S. (1981). *Am. Ceram. Soc. Bull.* **60**, poster 45-B-81, p. 376.  
 Mather, G. C., Dussarrat, C., Etourneau, J. & West, A. R. (2000). *J. Mater. Chem.* **10**, 2219–2230.  
 Miao, C. R. & Torardi, C. C. (1999). *J. Solid State Chem.* **145**, 110–115.  
 Rigaku (1999). *RAPID-AUTO*. Manual No. MJ13159A01. Rigaku Corporation, Tokyo, Japan.  
 Roth, R. S. (1984). *J. Solid State Chem.* **51**, P403–404.  
 Zachariasen, W. H. (1968). *Acta Cryst.* **A24**, 212–216.  
 Zocchi, M., Gatti, M., Santoro, A. & Roth, R. S. (1983). *J. Solid State Chem.* **48**, 420–430.  
 Zocchi, M., Gatti, M., Santoro, A. & Roth, R. S. (1984). *J. Solid State Chem.* **53**, 277–278.